Examination of retinal vascular trajectory in schizophrenia and bipolar disorder

Abhishek Appaji, MTech, ME [1,2†] Bhargavi Nagendra, DNB,[3†] Dona M. Chako, MPhil,[3] Ananth Padmanabha, MTech,[1] Arpitha Jacob, MPhil,[3] Chaitra V. Hiremath, DPM,[3] Shivarama Varambally, MD,[3] Muralidharan Kesavan, MD,[3] Ganesan Venkatasubramanian, MD, PhD,[3] Shyam V. Rao, PhD,[1,2] Carroll A. B. Webers, MD, PhD, FEBOpht,[2] Tos T. J. M. Berendschot, PhD[2] and Naren P. Rao, MD [3*]

Aim: Evidence suggests microvascular dysfunction (wider retinal venules and narrower arterioles) in schizophrenia (SCZ) and bipolar disorder (BD). The vascular development is synchronous with neuronal development in the retina and brain. The retinal vessel trajectory is related to retinal nerve fiber layer thinning and cerebrovascular abnormalities in SCZ and BD and has not yet been examined. Hence, in this study we examined the retinal vascular trajectory in SCZ and BD in comparison with healthy volunteers (HV).

Methods: Retinal images were acquired from 100 HV, SCZ patients, and BD patients, respectively, with a non-mydriatic fundus camera. Images were quantified to obtain the retinal arterial and venous trajectories using a validated, semiautomated algorithm. Analysis of covariance and regression analyses were conducted to examine group differences. A supervised machine-learning ensemble of bagged-trees method was used for automated classification of trajectory values.

Results: There was a significant difference among groups in both the retinal venous trajectory (HV: 0.17 ± 0.08; SCZ: 0.25 ± 0.17; BD: 0.27 ± 0.20; $P < 0.001$) and the arterial trajectory (HV: 0.34 ± 0.15; SCZ: 0.29 ± 0.10; BD: 0.29 ± 0.11; $P = 0.003$) even after adjusting for age and sex ($P < 0.001$). On post-hoc analysis, the SCZ and BD groups differed from the HV on retinal venous and arterial trajectories, but there was no difference between SCZ and BD patients. The machine learning showed an accuracy of 86% and 73% for classifying HV versus SCZ and BD, respectively.

Conclusion: Smaller trajectories of retinal arteries indicate wider and flatter curves in SCZ and BD. Considering the relation between retinal/cerebral vasculatures and retinal nerve fiber layer thinness, the retinal vascular trajectory is a potential marker for SCZ and BD. As a relatively affordable investigation, retinal fundus photography should be further explored in SCZ and BD as a potential screening measure.

Keywords: bipolar disorder, machine learning, retinal nerve fiber layer, retinal vascular trajectory, schizophrenia.

http://onlinelibrary.wiley.com/doi/10.1111/pcn.12921/full

The retina, an embryonic extension of the central nervous system, is often considered as a 'window to the brain' due to its easy accessibility.[1] Retinal imaging is a safer, faster, and less expensive technique compared to other imaging modalities, like magnetic resonance imaging (MRI), used for psychiatric disorders.[2] The retinal nerve fiber layer (RNFL), which is composed of axons from the retinal ganglion cells, shares an embryonic origin with the brain, thus permitting surrogate examination of axonal histopathology.[3] Studies have reported thinning of the RNFL as measured by optical coherence tomography (OCT) in several neuropsychiatric conditions.[1,3] RNFL thinning has also been found to be associated with brain atrophy in multiple sclerosis, validating its use as a marker for brain abnormality.[4] Several studies in the last decade have reported RNFL thinning in patients with schizophrenia (SCZ) and bipolar disorder (BD)[5–9] but not in major depressive disorder,[10,11] suggesting that RNFL abnormalities are limited to SCZ and BD. A recent study has also reported an overlap in genes implicated in macular thickness and systemic diseases, including SCZ.[12] Two genetic loci, rs7432375 and rs7523273, are

associated with risk for both age-related macular degeneration and SCZ.[13–15] Though the functional significance of these genes in the pathogenesis of SCZ is not completely known, it is interesting to note that rs7523273 is associated with functional brain activation in the precuneus/posterior cingulate cortex of SCZ patients.[16] Hence, though preliminary, these findings suggest a pleiotropy effect of these genes between RNFL thickness and SCZ.

However, the measurement of RNFL thickness requires OCT.[17] Though less expensive than brain imaging, the cost of OCT still limits its utility in the wider community under resource-constrained settings. Fundus imaging is less expensive than OCT and ideally suited for use in community settings. An earlier study reported a significant association between the retinal arterial trajectory measured as retinal artery angle (angle between the supratemporal and infratemporal arteries) and RNFL thickness.[18] This contribution to RNFL thickness by retinal blood vessels could either be direct or indirect and may be bidirectional. Another earlier study suggested that blood vessels directly contribute to the interindividual variations in

[1] Department of Medical Electronics, B. M. S. College of Engineering, Bangalore, India
[2] University Eye Clinic Maastricht, Maastricht University, Maastricht, The Netherlands
[3] Department of Psychiatry, National Institute of Mental Health and Neurosciences, Bangalore, India
* Correspondence: Email: docnaren@gmail.com
† Both authors contributed equally to the manuscript.

RNFL thickness in healthy individuals and patients.[19,20] In addition to this direct contribution, because the development of retinal vessels is influenced by axonal distribution, the locations of blood vessels influence the variations in RNFL thickness.[19,20]

The retinal arterial trajectory can be measured using a relatively inexpensive fundus camera,[21,22] and this provides an opportunity to indirectly examine abnormalities in RNFL thickness.

Former studies using fundus cameras have reported abnormalities in retinal vasculature; venular calibers were found to be increased in SCZ patients and in unaffected co-twins of SCZ patients.[23–25] Recently, we also reported wider venules and narrower arterioles in SCZ and BD patients compared to healthy volunteers (HV).[26] The trajectories of retinal vessels in SCZ and BD patients are yet to be examined, despite their relations with RNFL abnormalities. Hence, in this study we examined retinal vessel trajectory in patients with SCZ and BD in comparison with HV. Based on the literature suggestive of RNFL thinning in SCZ and BD, we hypothesized that these patients would have wider retinal arterial trajectories (in other words flatter curve, with the arms of the curve farther from the fovea) when compared to HV. Several lines of research in the past decade have suggested considerable overlap in the genetic and pathogenic factors across SCZ and BD; though there are a few differences between these two disorders, it is interesting to note that there are considerable similarities as well.[27] Considering these similarities between SCZ and BD, our secondary hypothesis was that there would be no significant difference in retinal arterial trajectories between these two groups. In addition, a proof-of-concept machine-learning method using an ensemble of bagged trees was employed for automated classification of patients and HV based on their vascular trajectory values.

Methods

Subjects

One hundred patients with SCZ and BD, respectively, were recruited from the clinical services of the National Institute of Mental Health and Neurosciences, Bangalore, India. Patients were examined by a board-certified psychiatrist and diagnosed as per the ICD-10.[28] Patients who had an ongoing psychiatric comorbidity, or had had substance abuse or dependence (except nicotine) in the previous 12 months were excluded from the study. One hundred HV were recruited using flyers and word of mouth from the same geographical area. None of the HV had a lifetime history of psychiatric disorder, neurological illness, or family history of psychoses in first-degree relatives. All HV were interviewed by a qualified psychiatrist and also completed the Cross-Cutting Symptom Scale[29,30] to rule out any Axis I disorders. Participants diagnosed or treated for hypertension, diabetes, stroke, or history of eye surgery/trauma were excluded from the study. The patients and HV were also excluded for other ophthalmologic disorders, such as macular degeneration and glaucoma, based on their medical history. Ophthalmic examinations, including refraction, axial length, and intraocular pressure, were not carried out. All participants were adults, aged 18 to 50 years. The study was approved by the institute ethics board and all participants provided written informed consent.

Clinical assessments

The severity of positive symptoms, negative symptoms, and general psychopathology in SCZ was measured using the Brief Psychiatric Rating Scale (BPRS).[31] In BD, the severity of clinical symptoms was measured using Young's Mania Rating Scale (YMRS)[32] and the Hamilton Depression Rating Scale (HDRS).[33] Functioning was assessed using the Global Assessment of Functioning (GAF)[34] and the Clinical Global Impression (CGI)[35] in both SCZ and BD.

Retinal image acquisition

The procedure of retinal image acquisition was explained to those who agreed to participate in the study and signed a consent form. They were seated in a dark room for 5 min prior to the procedure to facilitate auto-dilation of pupils through accommodation. Optic-disk-centered retinal images of both the eyes were acquired with a valid method by a trained individual using a fundus camera with a 40-degree field of view.[36] The retinal images were acquired using a non-mydriatic 3Nethra device (Forus Health, Bangalore, India) by an experienced operator. Each participant was asked to sit in front of the fundus camera and to rest his/her chin on its chin rest. The camera was adjusted to acquire the left eye retina by flashing a light and the image was captured and saved in the computer. This image-acquisition method was based on fundus illumination through light flashes forming a color image. The same procedure was repeated for the right eye.[26]

Measurement of trajectory of retinal vessels

All images were visually examined by a board-certified ophthalmologist and pathological conditions of the retina, such as macular degeneration and glaucoma, were ruled out. Experienced raters differentiated the vessels as arteries and veins using an established method.[37] The following criteria were used to differentiate the arteries and veins in accord with previous studies: (i) arteries are brighter in color than veins; (ii) arteries have a smaller caliber than veins; (iii) the central reflex (the light reflex of the inner parts of the vessel) is wider in arteries and narrower in veins; and (iv) arteries and veins usually alternate near the optic disk before branching out. The trajectories of arteries and veins for both the eyes were calculated using a validated mathematical model described in a previous study.[38] A semiautomated software was formulated using MATLAB 2018a (MathWorks, Natick, MA, USA). Initially, the retinal images of the right and left eyes were rotated 90° clockwise and anticlockwise, respectively. Following this, a minimum of 20 points were marked on the vascular trajectories passing through the infratemporal and supratemporal margin areas of the retinal images such that each arm to the right and left of the optic disk had a minimum of 10 points each (shown in Fig. 1). The infratemporal and supratemporal margins/peaks of the optic disk were chosen in view of the thick retinal nerve fiber bundles in this area. The fovea is located between these two peaks/margins, so the retina stretches more horizontally and/or vertically in some eyes due to tension on the fovea, resulting in a greater distance between these two peaks where the retinal vessel trajectories are measured. This results in a thinner retina.[38,39] The x and y coordinates of the marked points were automatically detected in MATLAB and were converted to new coordinates by shifting the origin to the center of the optic disk. Thereafter, these data of converted coordinates were fitted to a second-degree polynomial $\left(\frac{P_1 X^2}{100} + P_2 X + P_3 \right)$ curve-fitting equation based on the best-fit second-degree polynomial by the least-squares method as shown in Figure 1. In cases where the retinal artery or vein were branched, and the main artery was larger than the branch artery, the main artery was plotted for the trajectory. However, if the branch artery was as large as the main artery, marking was not done beyond the branching point. In such cases, also, a minimum of 20 points were marked. Under these conditions, a larger P_1 indicated that the curve of the retinal vascular trajectory was steeper and narrower, and that the arms of the curve would be closer to the fovea. A smaller P_1 indicated that the curve of the trajectory was flatter and wider, and the arms of the curve would be farther from the fovea. Hence, the value of P_1 was used as a single measure of the retinal vascular trajectory to indicate the steepness and width of the trajectory parabola. The average of the retinal vascular trajectories of the right and left eyes was used as the primary outcome measure. The procedure described above was adopted for both retinal arteries and veins separately. A subsample of 30 participant images was analyzed by two independent evaluators to check interrater reliability. A good interrater reliability of 0.83 (intraclass correlation for average artery: kappa = 0.85; $P < 0.001$; for average vein: Kappa = 0.81; $P < 0.001$) was obtained for the vascular trajectories.

Statistical analysis

All statistical analyses were performed using SPSS version 24 (IBM, Armonk, NY, USA). The Shapiro–Wilk test was used to examine the
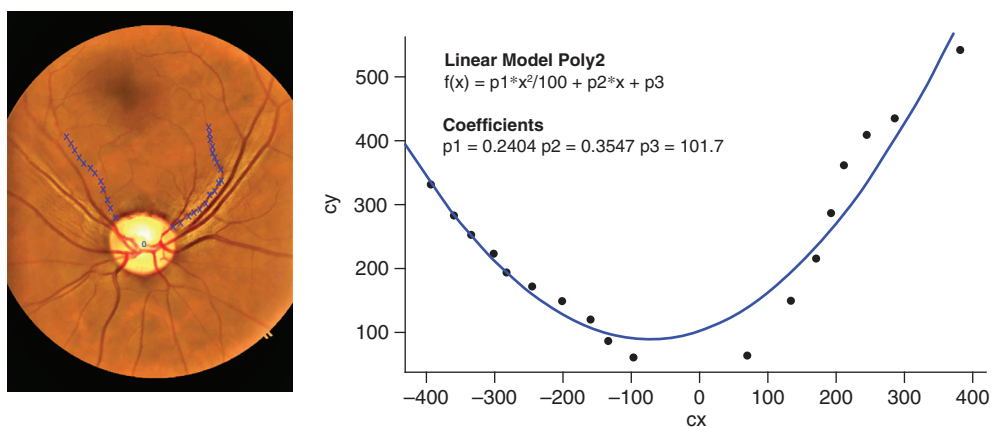
data for normative distribution. Parametric statistical tests were used as the data were found to be normatively distributed. Differences in age and sex distribution across the groups were analyzed using one-way analysis of variance (ANOVA) and the χ^2-test, respectively. Differences in retinal vascular trajectory across the groups were measured using analysis of covariance (ANCOVA). As we compared trajectories of both retinal arteries and veins, we applied the Bonferroni correction for multiple comparisons (three groups and two measures) and considered a corrected P-value of $\leq 0.05/6 = 0.0083$ to be significant. The contribution of age and sex as potential confounding variables was assessed using regression coefficients with 95% confidence interval between the groups, both with and without these as covariates. The relation between retinal trajectories and clinical/demographic variables was assessed using Pearson's correlation analyses using the scores on BPRS, YMRS, and HDRS, as well as age at onset of illness, duration of illness, and chlorpromazine-equivalent of antipsychotic as predictor variables. A P-value of <0.01 was considered significant in view of the multiple variables. To control for the confounding effects of nicotine dependence, a subanalysis was performed after excluding 12 subjects with SCZ and four subjects with BD who had nicotine dependence.

Machine-learning analysis

We conducted a proof-of-concept machine-learning analysis to examine the utility of retinal vascular measures in differentiating the three groups. The machine-learning algorithm was implemented through MATLAB 2018a using a supervised machine-learning approach. The labels used for training were based on the three groups (SCZ, BD, and HV). A total of six features from both the left and right eye were used for classification, namely, left and right retinal arterial trajectories, left and right retinal venous trajectories, and their respective averages. The supervised machine-learning model was created by

feeding a known set of input data (features) and the known group of the data (i.e., labels or classes). This model was then used to classify the new unknown data into one of the three groups through cross-validation. We used five default folds that partitioned the data into five disjoint sets; each fold trains the model using out-of-fold observations and assesses model performance using in-fold data followed by calculation of the average test error of overall folds. The data were partitioned into five equal folds out of which four folds were taken for training and one fold was taken for testing/validation. This process was repeated five times with each fold being used exactly once as the validation fold. This validation model was chosen to avoid overfitting of the data. The method provides good predictive accuracy to the final model trained using all the data. The usage of multiple fits ensures efficient use of all the available data despite small numbers. The learning rate was chosen as 0.1. The bagged decision trees ensemble method was used for classification. We also conducted a support-vector machine (SVM) analysis to independently confirm the findings. We chose SVM and the ensemble of bagged trees as these methods have good speed, high model flexibility, and can be implemented with moderate computational power,[40,41] translating to feasibility in real life clinical scenarios.

Results
Comparison of demographic variables
Out of the 300 participants recruited, 31 were excluded following quality check of retinal images and ambiguity in retinal vascular trajectory marking. Thus, 87 HV, 94 SCZ, and 88 BD were included for the analysis, totaling 269 participants. Demographic details and clinical measures are provided in Table 1. We found a significant difference in age ($P = 0.005$) across the three groups and no difference in sex distribution ($P = 0.053$).

Table 1. Comparison of demographic and clinical details between the groups

	HV ($n = 87$)	SCZ ($n = 94$)	BD ($n = 88$)	$F/t/\chi^2$	P
Age (years)	30.2 ± 7.6	32.5 ± 6.0	33.4 ± 6.0	5.4	0.005
Sex ratio (M/F)	41/46	61/33	51/37	5.87	0.053
Age at onset (years)	—	25.0 ± 5.2	23.8 ± 6.0	1.7	0.196
Duration of illness (years)	—	7.6 ± 5.2	9.1 ± 5.6	2.6	0.11
BPRS	—	25.83 ± 5.4	—	—	—
HDRS	—	—	3.97 ± 5.6	—	—
YMRS	—	—	1.75 ± 2.9	—	—

BD, bipolar disorder patients; BPRS, Brief Psychiatric Rating Scale; F, analysis of variance; HDRS, Hamilton Depression Rating Scale; HV, healthy volunteer; SCZ, schizophrenia patients; t, independent t-test; YMRS, Young's Mania Rating Scale.

Differences in trajectory of retinal vessels between HV and patients

ANCOVA showed a significant difference across the three groups in trajectories of retinal artery (constant P_1 of HV: 0.34 ± 0.15; SCZ: 0.29 ± 0.10; BD: 0.29 ± 0.11; $F = 4.1$; $P = 0.003$). The results showed that the value P_1 of the retinal arterial trajectory was significantly smaller in SCZ (0.29 ± 0.10) and BD (0.29 ± 0.11) patients as compared to HV (0.34 ± 0.15), indicating flatter and wider retinal arterial trajectories in patients. There was a significant difference across the three groups in the trajectories of retinal veins as well (constant P_1 of HV: 0.17 ± 0.08; SCZ: 0.25 ± 0.17; BD: 0.27 ± 0.20; $F = 5.2$; $P < 0.001$). However, the value P_1 of the retinal venous trajectory was significantly greater in SCZ (0.25 ± 0.17) and BD (0.27 ± 0.20) patients as compared to HV (0.17 ± 0.08), indicating steeper and narrower retinal venous trajectories in patients. Post-hoc analysis revealed that while there was a significant difference between HV and both SCZ and BD patients in the trajectories of retinal arteries ($P < 0.01$) and veins ($P < 0.01$), there was no significant difference between the two patient groups, SCZ and BD ($P > 0.05$), on these measures (Fig. S1 and Table S1).

The contribution of age and sex as potential confounding variables was assessed using regression analysis. There was no considerable difference in the regression coefficients and significance values either with or without age and sex as additional regressors on separate linear regression analyses (Table 2), suggesting the absence of any significant effect of these potential confounders. Further details are provided in Table S2. Similarly, nicotine dependence did not show significant effects either (Appendix S1).

Relation between clinical variables and retinal vascular trajectory

There was no significant correlation between clinical variables (duration of illness, age at onset, total score on YMRS, HDRS, BPRS, and antipsychotic dose) and trajectories of retinal arteries and veins ($P > 0.01$) on Pearson's partial correlation analyses with and without age and sex as covariates (Table S3).

Machine-learning analyses

Ensemble of bagged trees had an accuracy of 86% with sensitivity of 88% and specificity of 85% for differentiating HV and SCZ. A lower but considerably good accuracy of 73% with sensitivity of 78% and specificity of 76% was obtained for differentiating HV and BD. For differentiating SCZ and BD, the accuracy was 77% with a sensitivity of 81% and specificity of 86%. The exploratory SVM analysis showed a similar, but relatively lesser, accuracy than the ensemble of bagged trees (Appendix S2).

Discussion

This is the first study to assess the trajectories of retinal vessels in SCZ and BD patients in comparison with HV. The results show that P_1 of the retinal arterial trajectory was significantly lesser and P_1 of the retinal venous trajectory was significantly greater in SCZ and BD patients as compared to HV. This indicates a wider and flatter parabola of the arteries and steeper and narrower parabola of the veins in the patients than in the HV. Neither the arterial nor venous trajectories differed between patients with SCZ and those with BD.

Our findings of wider retinal arterial trajectories are in accord with our hypothesis and previous findings. During embryonic development, common mechanisms underlie the vascularization of both the retina and the brain as the retina is embryologically an extension of the diencephalon.[42] In both the retina and the brain, the vascular development is synchronous to neuronal development; the neurovascular coupling assures simultaneous generation of neuroblasts and blood vessels.[43] In addition, endothelial cells play a critical role in migration and differentiation of oligodendrocytes.[43] Interestingly, emerging evidence suggests the role of angiogenesis and blood vessel pathologies in the pathogenesis of psychoses, importantly SCZ. Preliminary evidence from genetic, post-mortem, and imaging studies suggests a vascular remodeling and hypoxia signaling as risk factors for SCZ.[43,44] Considering these relations, it is possible that retinal vascular abnormalities are indicative of cerebral vascular abnormalities, which in turn are implicated in the pathogenesis of psychoses.

In addition, the retinal arterial trajectory measured as the retinal artery angle has been shown to have significant association with thinner RNFL[18] and several studies have reported wider retinal artery trajectories to be associated with RNFL defects.[38,39,45,46]

A few studies have examined RNFL thickness using OCT in SCZ and BD patients and have reported thinning of the RNFL[5,9,47–49] and the inner nuclear layer[50] in patients compared to HV.

Hence, our findings of wider retinal artery trajectories in SCZ and BD patients suggest that the retinal arterial trajectory could be a potential surrogate measure of RNFL thickness seen in psychoses. Our findings provide rationale for further examination of the association between retinal vascular trajectory and RNFL thickness using OCT in SCZ and BD.

Based on the common developmental origins between the retina and the brain,[51] a few studies have examined the relation between RNFL thickness and brain structure. In a large population-based study, a thinner RNFL and ganglion cell layer was shown to be associated with lower gray matter density in the visual cortex and a thinner ganglion cell layer was associated with lower gray matter density in the thalamus.[51] In addition, lower fractional anisotropy of the corpus callosum and optic radiation were associated with thinner RNFL.[51,52] While the definitive mechanisms are still unclear, axonal degeneration has been postulated to be responsible for both thinning of the RNFL and decreased gray matter volume in the brain.[53] However, the brain correlates of thin RNFL have not directly been examined in SCZ and BD to date. Considering the relation between retinal arterial trajectory and RNFL thickness, it is possible that the abnormalities in retinal vascular trajectory may also be related to the

Table 2. Mean difference of retinal trajectories among HV, SCZ patients, and BD patients adjusted for age and sex

Parameter	Group		Not adjusted for age and sex		Adjusted for age and sex	
			β† (95%CI)	P	β† (95%CI)	P
Retinal vein trajectory	HV	SCZ	0.08 (0.041 to 0.119)	<0.001	0.075 (0.035 to 0.115)	<0.001
	HV	BD	0.102 (0.041 to 0.119)	<0.001	0.107 (0.06 to 0.153)	<0.001
	SCZ	BD	0.022 (−0.031 to 0.076)	0.417	0.022 (−0.032 to 0.076)	0.415
Retinal artery trajectory	HV	SCZ	−0.058 (−0.096 to −0.019)	0.003	−0.049 (−0.088 to −0.010)	0.014
	HV	BD	−0.056 (−0.096 to −0.016)	0.006	−0.042 (−0.083 to −0.002)	0.041
	SCZ	BD	0.002 (−0.030 to 0.033)	0.915	0.00 (−0.031 to 0.032)	0.985

†Regression coefficient.
BD, bipolar disorder patients; CI, confidence interval; HV, healthy volunteers; SCZ, schizophrenia patients.

structural brain abnormalities seen in SCZ and BD.[54–56] However, this speculation is based on indirect evidence as the relation between retinal vascular trajectory and brain structure/function in SCZ or BD remains to be explored.

While several studies have examined retinal arterial trajectories, retinal venous trajectories have taken the backseat. Our findings suggest an inverse relation between the trajectories of retinal arteries and veins between the groups. This finding is similar to the inverse relation seen in retinal vascular caliber; while patients with psychoses had narrower arterioles than HV, they had wider venules.[26] In the absence of joint examination of retinal venous trajectory and RNFL, definitive conclusions cannot be drawn regarding the reasons or pathophysiological mechanisms behind the differential findings across the arteries and veins. Studies employing multimodal examination using fundus photography, OCT, and magnetic resonance imaging in SCZ and BD patients are needed for direct evidence and definitive understanding of these relations.

Our secondary aim was to examine the utility of machine-learning techniques to differentiate patients from HV using retinal vessel trajectory as the input variable. Several studies have used the machine-learning approach to classify SCZ/BD and HV using neuroimaging/electrophysiologic/cognitive data as input variables.[57–61] A recent study reported prediction accuracy of 76% to differentiate SCZ from HV using a multisite machine-learning analysis.[62] Another study reported use of machine-learning analysis and structural MRI to differentiate treatment nonresponders from treatment responders with a sensitivity of 71% and specificity of 68%.[63] Similar to structural imaging, functional imaging is also used to classify SCZ and HV; a recent study using a functional connectivity measure reported an accuracy of 75% with a sensitivity of 74% and specificity of 84%.[64] While several studies have examined the use of the machine-learning approach in SCZ, it is relatively less examined in BD. A few studies using neuroimaging measures have reported an accuracy of 70%–80% to classify BD and HV.[65] A higher accuracy of 95% was reported to classify BD and HV using a combination of neuropsychological tests and plasma markers.[66] On the other hand, a few studies have explored the utility of machine-learning analyses using retinal images in ophthalmology.[67–71] The machine-learning approach has been successfully used to classify healthy versus diabetic retinopathy, age-related macular degeneration, glaucoma, retinopathy of prematurity, and so forth.[72–74] Ours is the first study to utilize machine-learning analysis to differentiate SCZ/BD from HV using retinal vessel trajectory as the input factor. Findings of our study provide proof of concept to use machine-learning techniques using retinal vessel trajectory as an input factor to classify SCZ/BD and HV. The ensemble of bagged trees method of classification crossed the critical threshold of more than 80% for classifying HV and SCZ.[75,76] However, our sample size being small, these findings need to be replicated in future studies with larger samples.

A few limitations should be considered in relation to our study findings. All patients were on treatment with medication and the confounding effect of pharmacotherapy cannot be ruled out. However, as shown in Table S3, there was no significant correlation between retinal vessel trajectories and chlorpromazine dose equivalents, suggesting absence of significant effect of antipsychotics. Future studies with a subsample of drug-naïve subjects can control for this confounder. The representation of BD-I and BD-II patients were not uniform. There were 65 patients with BD-I and the rest had BD-II. Considering the small number of participants in each subgroup, we could not examine whether the subtypes of BD differ on these parameters. Future studies with larger samples including BD-I and BD-II patients are needed for the same. The groups were not age-matched. However, even after controlling for age, the results remained significant. As shown in Table 2, the regression coefficients were comparable both with and without age and sex as covariates. Sixteen patients had nicotine dependence (four BD and 12 SCZ), which could have confounded the results considering that previous studies have reported an association between long-term nicotine use and RNFL thickness.[77,78] However, as nicotine dependence is a common comorbidity in schizophrenia,[79] exclusion of patients with

nicotine use would have affected the generalizability of findings. It is important to note that the differences between groups remained significant even after excluding these 16 participants (details in Appendix 2). We measured blood pressure, body mass index, and/or glucose levels of some, but not all, of the participants on the examination day. Though participants were young and those with a history of hypertension or diabetes mellitus were excluded, one cannot rule out the possibility of undiagnosed hypertension or diabetes mellitus. To control for the potential confound, we measured blood pressure and body mass index in a subgroup of patients and conducted a subanalysis including these measures. The results remained the same even after inclusion of these measures (details in Appendix S3). Future studies need to consider measurement of these parameters on the day of retinal image acquisition. Another major limitation of the study is that we did not measure other ophthalmologic parameters, including refraction, axial length, and intraocular pressure. It is important to note that ophthalmologic comorbidities are seen commonly in schizophrenia[80] and may have confounded the findings. Hence, it will be important to measure these parameters in the future. We did not measure the axial length of the eye or visual acuity/refraction, which could have influenced the retinal vascular trajectory measurements. However, it is important to note that a previous study has reported a significant association between the retinal arterial trajectory and RNFL thickness even after controlling for the axial length.[18] Moreover, another study has reported that SCZ patients and HV do not differ in axial length of the eye or disorders of refraction.[81] Hence, axial length is not likely to have significant confounding effects on the findings. However, it would be ideal if future studies concurrently measured the axial length and refraction to correct for their effects.

Our study findings have important implications. Retinal vascular abnormalities bear relation to abnormalities in RNFL thickness, which in turn is related to brain abnormalities seen in SCZ and BD.[82,83] Fundus photography is relatively inexpensive when compared to OCT or neuroimaging. In addition, the portable nature of the equipment also makes it an ideal tool for use in peripheral centers or where resources are limited. These advantages of fundus photography, together with our findings from machine-learning analysis, indicate the potential utility of this method in wider, resource-constrained settings and warrant further studies with larger sample sizes. Machine-learning analysis with the use of a single measure (retinal vessel trajectory) demonstrated reasonable accuracy despite the potential confounding factors, suggesting its potential utility as a clinical marker.[84] Considerable increase in accuracy may be obtained with increase in sample size along with dynamic learning and deep learning. These preliminary findings provide sufficient rationale for future studies along similar lines on larger samples.

Conclusions

The findings of our study indicate significant differences between the retinal vessel trajectories in patients (SCZ and BD) and HV. Both SCZ and BD patients, compared to HV, had smaller P_1 for arterial trajectories, indicating flatter and wider curves of retinal arteries. As retinal fundoscopic imaging is affordable, accessible, and easy to perform, it could prove to be useful as a surrogate investigation for the RNFL thinning seen in SCZ and BD. The findings from machine-learning analysis provide proof of concept and preliminary support towards its potential to differentiate patients with SCZ and BD from HV. Future studies need to consider examining the relation between retinal vascular trajectory and RNFL using OCT. Also, the relation between retinal vascular trajectory and brain structure and function need to be considered in the future.

Disclosure statement

Dr Shyam V. Rao is the Co-founder and Director at Forus Health Pvt. Ltd., India. The other authors report no conflicts of interest.

Author contributions

References

1. Schonfeldt-Lecuona C, Kregel T, Schmidt A *et al*. From imaging the brain to imaging the retina: Optical coherence tomography (OCT) in schizophrenia. *Schizophr. Bull.* 2016; **42**: 9–14.
2. Patton N, Aslam T, Macgillivray T, Pattie A, Deary IJ, Dhillon B. Retinal vascular image analysis as a potential screening tool for cerebrovascular disease: A rationale based on homology between cerebral and retinal microvasculatures. *J. Anat.* 2005; **206**: 319–348.
3. London A, Benhar I, Schwartz M. The retina as a window to the brain: From eye research to CNS disorders. *Nat. Rev. Neurol.* 2013; **9**: 44–53.
4. Gordon-Lipkin E, Chodkowski B, Reich DS *et al*. Retinal nerve fiber layer is associated with brain atrophy in multiple sclerosis. *Neurology* 2007; **69**: 1603–1609.
5. Lee WW, Tajunisah I, Sharmilla K, Peyman M, Subrayan V. Retinal nerve fiber layer structure abnormalities in schizophrenia and its relationship to disease state: Evidence from optical coherence tomography. *Invest. Ophthalmol. Vis. Sci.* 2013; **54**: 7785–7792.
6. Yilmaz U, Kucuk E, Ulgen A *et al*. Retinal nerve fiber layer and macular thickness measurement in patients with schizophrenia. *Eur. J. Ophthalmol.* 2016; **26**: 375–378.
7. Garcia-Portilla MP, Garcia-Alvarez L, de la Fuente-Tomas L *et al*. Could structural changes in the retinal layers be a new biomarker of mental disorders? A systematic review and thematic synthesis. *Rev. Psiquiatr. Salud. Ment.* 2019; **12**: 116–129.
8. Samani NN, Proudlock FA, Siram V *et al*. Retinal layer abnormalities as biomarkers of schizophrenia. *Schizophr. Bull.* 2018; **44**: 876–885.
9. Silverstein SM, Paterno D, Cherneski L, Green S. Optical coherence tomography indices of structural retinal pathology in schizophrenia. *Psychol. Med.* 2018; **48**: 2023–2033.
10. Sonmez I, Kosger F, Aykan U. Retinal nerve fiber layer thickness measurement by spectral-domain optical coherence tomography in patients with major depressive disorder. *Noro Psikiyatr. Ars.* 2017; **54**: 62–66.
11. Yildiz M, Alim S, Batmaz S *et al*. Duration of the depressive episode is correlated with ganglion cell inner plexifrom [sic] layer and nasal retinal fiber layer thicknesses: Optical coherence tomography findings in major depression. *Psychiatry Res. Neuroimaging* 2016; **251**: 60–66.
12. Gao XR, Huang H, Kim H. Genome-wide association analyses identify 139 loci associated with macular thickness in the UK Biobank cohort. *Hum. Mol. Genet.* 2018; **28**: 1162–1172.
13. Grassmann F, Kiel C, Zimmermann ME *et al*. Genetic pleiotropy between age-related macular degeneration and 16 complex diseases and traits. *Genome Med.* 2017; **9**: 29.
14. Jaffe AE, Straub RE, Shin JH *et al*. Developmental and genetic regulation of the human cortex transcriptome illuminate schizophrenia pathogenesis. *Nat. Neurosci.* 2018; **21**: 1117–1125.
15. Ohi K, Shimada T, Yasuyama T, Uehara T, Kawasaki Y. Variability of 128 schizophrenia-associated gene variants across distinct ethnic populations. *Transl. Psychiatry* 2017; **7**: e988.
16. Erk S, Mohnke S, Ripke S *et al*. Functional neuroimaging effects of recently discovered genetic risk loci for schizophrenia and polygenic risk profile in five RDoC subdomains. *Transl. Psychiatry* 2017; **7**: e997.
17. Costa RA, Skaf M, Melo LA Jr *et al*. Retinal assessment using optical coherence tomography. *Prog. Retin. Eye Res.* 2006; **25**: 325–353.
18. Yamashita T, Asaoka R, Tanaka M *et al*. Relationship between position of peak retinal nerve fiber layer thickness and retinal arteries on sectoral retinal nerve fiber layer thickness. *Invest. Ophthalmol. Vis. Sci.* 2013; **54**: 5481–5488.
19. Hood DC, Salant JA, Arthur SN, Ritch R, Liebmann JM. The location of the inferior and superior temporal blood vessels and inter-individual variability of the retinal nerve fiber layer thickness. *J. Glaucoma* 2010; **19**: 158–166.
20. Hood DC, Fortune B, Arthur SN *et al*. Blood vessel contributions to retinal nerve fiber layer thickness profiles measured with optical coherence tomography. *J. Glaucoma* 2008; **17**: 519–528.
21. Gupta S, Zivadinov R, Ramanathan M, Weinstock-Guttman B. Optical coherence tomography and neurodegeneration: Are eyes the windows to the brain? *Expert Rev. Neurother.* 2016; **16**: 765–775.
22. Thomson KL, Yeo JM, Waddell B, Cameron JR, Pal S. A systematic review and meta-analysis of retinal nerve fiber layer change in dementia, using optical coherence tomography. *Alzheimers Dement.* 2015; **1**: 136–143.
23. Meier MH, Shalev I, Moffitt TE *et al*. Microvascular abnormality in schizophrenia as shown by retinal imaging. *Am. J. Psychiatry* 2013; **170**: 1451–1459.
24. Meier MH, Gillespie NA, Hansell NK *et al*. Retinal microvessels reflect familial vulnerability to psychotic symptoms: A comparison of twins discordant for psychotic symptoms and controls. *Schizophr. Res.* 2015; **164**: 47–52.
25. Naiberg MR, Hatch JK, Selkirk B *et al*. Retinal photography: A window into the cardiovascular-brain link in adolescent bipolar disorder. *J. Affect. Disord.* 2017; **218**: 227–237.
26. Appaji A, Nagendra B, Chako DM *et al*. Retinal vascular abnormalities in schizophrenia and bipolar disorder: A window to the brain. *Bipolar Disord.* 2019. https://doi.org/10.1111/bdi.12779
27. Murray RM, Sham P, Van Os J, Zanelli J, Cannon M, McDonald C. A developmental model for similarities and dissimilarities between schizophrenia and bipolar disorder. *Schizophr. Res.* 2004; **71**: 405–416.
28. Sheehan DV, Lecrubier Y, Sheehan KH *et al*. The Mini-International Neuropsychiatric Interview (M.I.N.I.): The development and validation of a structured diagnostic psychiatric interview for DSM-IV and ICD-10. *J. Clin. Psychiatry* 1998; **59**: 22–33; quiz 34–57.
29. Clarke DE, Kuhl EA. DSM-5 cross-cutting symptom measures: A step towards the future of psychiatric care? *World Psychiatry* 2014; **13**: 314–316.
30. Narrow WE, Clarke DE, Kuramoto SJ *et al*. DSM-5 field trials in the United States and Canada, part III: Development and reliability testing of a cross-cutting symptom assessment for DSM-5. *Am. J. Psychiatry* 2013; **170**: 71–82.
31. Overall JE, Gorham DR. The Brief Psychiatric Rating Scale. *Psychol. Rep.* 1962; **10**: 799–812.
32. Young RC, Biggs JT, Ziegler VE, Meyer DA. A rating scale for mania: Reliability, validity and sensitivity. *Br. J. Psychiatry* 1978; **133**: 429–435.
33. Hamilton M. A rating scale for depression. *J. Neurol. Neurosurg. Psychiatry* 1960; **23**: 56–62.
34. Jones SH, Thornicroft G, Coffey M, Dunn G. A brief mental health outcome scale-reliability and validity of the Global Assessment of Functioning (GAF). *Br. J. Psychiatry* 1995; **166**: 654–659.
35. Busner J, Targum SD. The Clinical Global Impressions Scale: Applying a research tool in clinical practice. *Psychiatry* 2007; **4**: 28–37.
36. Nguyen TT, Islam FM, Farouque HM *et al*. Retinal vascular caliber and brachial flow-mediated dilation: The multi-ethnic study of atherosclerosis. *Stroke* 2010; **41**: 1343–1348.
37. Kondermann C, Kondermann D, Yan M. Blood vessel classification into arteries and veins in retinal images. *Proc. SPIE 6512, Medical Imaging 2007: Image Processing* 2007: 651247.
38. Yamashita T, Sakamoto T, Terasaki H, Tanaka M, Kii Y, Nakao K. Quantification of retinal nerve fiber and retinal artery trajectories using second-order polynomial equation and its association with axial length. *Invest. Ophthalmol. Vis. Sci.* 2014; **55**: 5176–5182.
39. Yamashita T, Nitta K, Sonoda S, Sugiyama K, Sakamoto T. Relationship between location of retinal nerve fiber layer defect and curvature of retinal artery trajectory in eyes with normal tension glaucoma. *Invest. Ophthalmol. Vis. Sci.* 2015; **56**: 6190–6195.
40. Lupascu CA, Tegolo D, Trucco E. Accurate estimation of retinal vessel width using bagged decision trees and an extended multiresolution Hermite model. *Med. Image Anal.* 2013; **17**: 1164–1180.
41. Mbogning C, Perdry H, Broet P. A bagged, partially linear, tree-based regression procedure for prediction and variable selection. *Hum. Hered.* 2015; **79**: 182–193.
42. Hughes S, Yang H, Chan-Ling T. Vascularization of the human fetal retina: Roles of vasculogenesis and angiogenesis. *Invest. Ophthalmol. Vis. Sci.* 2000; **41**: 1217–1228.

43. Katsel P, Roussos P, Pletnikov M, Haroutunian V. Microvascular anomaly conditions in psychiatric disease. Schizophrenia - angiogenesis connection. *Neurosci. Biobehav. Rev.* 2017; **77**: 327–339.

44. Baruah J, Vasudevan A. The vessels shaping mental health or illness. *Open Neurol. J.* 2019; **13**: 1–9.

45. Yamashita T, Terasaki H, Yoshihara N, Kii Y, Uchino E, Sakamoto T. Relationship between retinal artery trajectory and axial length in Japanese school students. *Jpn. J. Ophthalmol.* 2018; **62**: 315–320.

46. Yoshihara N, Sakamoto T, Yamashita T *et al.* Wider retinal artery trajectories in eyes with macular hole than in fellow eyes of patients with unilateral idiopathic macular hole. *PLoS One* 2015; **10**: e0122876.

47. Mehraban A, Samimi SM, Entezari M, Seifi MH, Nazari M, Yaseri M. Peripapillary retinal nerve fiber layer thickness in bipolar disorder. *Graefes Arch. Clin. Exp. Ophthalmol.* 2016; **254**: 365–371.

48. Khalil MA, Saleh AA, Gohar SM, Khalil DH, Said M. Optical coherence tomography findings in patients with bipolar disorder. *J. Affect. Disord.* 2017; **218**: 115–122.

49. Chu EM, Kolappan M, Barnes TR, Joyce EM, Ron MA. A window into the brain: An in vivo study of the retina in schizophrenia using optical coherence tomography. *Psychiatry Res.* 2012; **203**: 89–94.

50. Garcia-Martin E, Gavin A, Garcia-Campayo J *et al.* Visual function and retinal changes in patients with bipolar disorder. *Retina* 2018. https://doi.org/10.1097/IAE.0000000000002252

51. Mutlu U, Ikram MK, Roshchupkin GV *et al.* Thinner retinal layers are associated with changes in the visual pathway: A population-based study. *Hum. Brain Mapp.* 2018; **39**: 4290–4301.

52. Scheel M, Finke C, Oberwahrenbrock T *et al.* Retinal nerve fibre layer thickness correlates with brain white matter damage in multiple sclerosis: A combined optical coherence tomography and diffusion tensor imaging study. *Mult. Scler.* 2014; **20**: 1904–1907.

53. Kalenderoglu A, Celik M, Sevgi-Karadag A, Egilmez OB. Optic coherence tomography shows inflammation and degeneration in major depressive disorder patients correlated with disease severity. *J. Affect. Disord.* 2016; **204**: 159–165.

54. Bellani M, Yeh PH, Tansella M, Balestrieri M, Soares JC, Brambilla P. DTI studies of corpus callosum in bipolar disorder. *Biochem. Soc. Trans.* 2009; **37**: 1096–1098.

55. Duarte JA, de Araujo ESJQ, Goldani AA, Massuda R, Gama CS. Neurobiological underpinnings of bipolar disorder focusing on findings of diffusion tensor imaging: A systematic review. *Rev. Bras. Psiquiatr.* 2016; **38**: 167–175.

56. Hibar DP, Westlye LT, Doan NT *et al.* Cortical abnormalities in bipolar disorder: An MRI analysis of 6503 individuals from the ENIGMA Bipolar Disorder Working Group. *Mol. Psychiatry* 2018; **23**: 932–942.

57. Zhao K, So HC. Drug repositioning for schizophrenia and depression/anxiety disorders: A machine learning approach leveraging expression data. *IEEE J. Biomed. Health Inform.* 2018; **23**: 1304–1315.

58. Tandon N, Tandon R. Will machine learning enable us to finally cut the Gordian knot of schizophrenia. *Schizophr. Bull.* 2018; **44**: 939–941.

59. Chung Y, Addington J, Bearden CE *et al.* Use of machine learning to determine deviance in neuroanatomical maturity associated with future psychosis in youths at clinically high risk. *JAMA Psychiatry* 2018; **75**: 960–968.

60. Mwangi B, Wu MJ, Bauer IE *et al.* Predictive classification of pediatric bipolar disorder using atlas-based diffusion weighted imaging and support vector machines. *Psychiatry Res.* 2015; **234**: 265–271.

61. Hajek T, Cooke C, Kopecek M, Novak T, Hoschl C, Alda M. Using structural MRI to identify individuals at genetic risk for bipolar disorders: A 2-cohort, machine learning study. *J. Psychiatry Neurosci.* 2015; **40**: 316–324.

62. Rozycki M, Satterthwaite TD, Koutsouleris N *et al.* Multisite machine learning analysis provides a robust structural imaging signature of schizophrenia detectable across diverse patient populations and within individuals. *Schizophr. Bull.* 2018; **44**: 1035–1044.

63. Mourao-Miranda J, Reinders AA, Rocha-Rego V *et al.* Individualized prediction of illness course at the first psychotic episode: A support vector machine MRI study. *Psychol. Med.* 2012; **42**: 1037–1047.

64. Ramkiran S, Sharma A, Rao NP. Resting-state anticorrelated networks in schizophrenia. *Psychiatry Res. Neuroimaging* 2019; **284**: 1–8.

65. Librenza-Garcia D, Kotzian BJ, Yang J *et al.* The impact of machine learning techniques in the study of bipolar disorder: A systematic review. *Neurosci. Biobehav. Rev.* 2017; **80**: 538–554.

66. Besga A, Gonzalez I, Echeburua E *et al.* Discrimination between Alzheimer's disease and late onset bipolar disorder using multivariate analysis. *Front. Aging Neurosci.* 2015; **7**: 231.

67. Saha SK, Fernando B, Cuadros J, Xiao D, Kanagasingam Y. Automated quality assessment of colour fundus images for diabetic

68. Roychowdhury S, Koozekanani DD, Parhi KK. DREAM: Diabetic retinopathy analysis using machine learning. *IEEE J. Biomed. Health Inform.* 2014; **18**: 1717–1728.

69. Ogunyemi O, Kermah D. Machine learning approaches for detecting diabetic retinopathy from clinical and public health records. *AMIA Annu. Symp. Proc.* 2015; **2015**: 983–990.

70. Bolon-Canedo V, Ataer-Cansizoglu E, Erdogmus D *et al.* Dealing with inter-expert variability in retinopathy of prematurity: A machine learning approach. *Comput. Methods Programs Biomed.* 2015; **122**: 1–15.

71. Omodaka K, An G, Tsuda S *et al.* Classification of optic disc shape in glaucoma using machine learning based on quantified ocular parameters. *PLoS One* 2017; **12**: e0190012.

72. Ting DSW, Pasquale LR, Peng L *et al.* Artificial intelligence and deep learning in ophthalmology. *Br. J. Ophthalmol.* 2019; **103**: 167–175.

73. Lee A, Taylor P, Kalpathy-Cramer J, Tufail AJO. Machine learning has arrived! *Ophthalmology* 2017; **124**: 1726–1728.

74. Gulshan V, Peng L, Coram M *et al.* Development and validation of a deep learning algorithm for detection of diabetic retinopathy in retinal fundus photographs. *JAMA* 2016; **316**: 2402–2410.

75. Savitz JB, Rauch SL, Drevets WC. Clinical application of brain imaging for the diagnosis of mood disorders: The current state of play. *Mol. Psychiatry* 2013; **18**: 528–539.

76. Nunes A, Schnack HG, Ching CRK *et al.* Using structural MRI to identify bipolar disorders - 13 site machine learning study in 3020 individuals from the ENIGMA Bipolar Disorders Working Group. *Mol. Psychiatry* 2018. https://doi.org/10.1038/s41380-018-0228-9

77. Ahuja S, Kumar PS, Kumar VP, Kattimani S, Akkilagunta S. Effect of chronic alcohol and tobacco use on retinal nerve fibre layer thickness: A case-control study. *BMJ Open Ophthalmol.* 2017; **1**: e000003.

78. Dervisogullari MS, Totan Y, Tenlik A, Yuce A, Guler E. Effect of smoking on retina nerve fiber layer and ganglion cell-inner plexiform layer complex. *Cutan. Ocul. Toxicol.* 2015; **34**: 282–285.

79. de Leon J, Diaz FJ. A meta-analysis of worldwide studies demonstrates an association between schizophrenia and tobacco smoking behaviors. *Schizophr. Res.* 2005; **76**: 135–157.

80. Silverstein SM, Rosen R. Schizophrenia and the eye. *Schizophr. Res. Cogn.* 2015; **2**: 46–55.

81. Cumurcu T, Keser S, Cumurcu BE, Gunduz A, Kartalci S. Refraction and eye anterior segment parameters in schizophrenic patients. *Arq. Bras. Oftalmol.* 2015; **78**: 180–184.

82. Pan J, Zhou Y, Xiang Y, Yu J. Retinal nerve fiber layer thickness changes in schizophrenia: A meta-analysis of case–control studies. *Psychiatry Res.* 2018; **270**: 786–791.

83. Lizano P, Bannai D, Lutz O, Kim LA, Miller J, Keshavan M. A meta-analysis of retinal cytoarchitectural abnormalities in schizophrenia and bipolar disorder. *Schizophr. Bull.* 2019. https://doi.org/10.1093/schbul/sbz029

84. Frank RA, Galasko D, Hampel H *et al.* Biological markers for therapeutic trials in Alzheimer's disease. *Neurobiol. Aging* 2003; **24**: 521–536.

Supporting information

Additional Supporting Information may be found in the online version of this article at the publisher's web-site:

Table S1. Post-hoc analysis of variance of retinal trajectory in the three groups

Table S2. Details of regression coefficient between groups with and without age and sex as predictor variables

Table S3. Relation between clinical variables and trajectory of retinal vessels

Appendix S1. Effect of nicotine use on retinal trajectory measurements

Appendix S2. Support-vector machine (SVM) performance for classification

Appendix S3. Relation between retinal vascular trajectory, body mass index, and blood pressure

Figure S1. Diagrammatic representation of group means of trajectory of retinal veins and retinal arteries.